Journal of Membrane Science 364 (2010) 233–241

Contents lists available at ScienceDirect

Journal of Membrane Science

journal homepage: www.elsevier.com/locate/memsci

Selection of inorganic-based draw solutions for forward osmosis applications

Andrea Achilli [a,*], Tzahi Y. Cath [b], Amy E. Childress [a]

[a] Department of Civil and Environmental Engineering, University of Nevada Reno, Reno, NV 89557, USA
[b] Division of Environmental Science and Engineering, Colorado School of Mines, Golden, CO 80401, USA

ARTICLE INFO

Article history:
Received 18 November 2009
Received in revised form 16 July 2010
Accepted 9 August 2010
Available online 14 August 2010

Keywords:
Osmosis
Forward osmosis
Draw solution
Concentration polarization
Reverse salt diffusion
Water and wastewater treatment

ABSTRACT

In this investigation, a protocol for the selection of optimal draw solutions for forward osmosis (FO) applications was developed and the protocol was used to determine the most appropriate draw solutions for specific FO applications using a currently available FO membrane. The protocol includes a desktop screening process and laboratory and modeling analyses. The desktop screening process resulted in 14 draw solutions suitable for FO applications. The 14 draw solutions were then tested in the laboratory to evaluate water flux and reverse salt diffusion through the FO membrane. Internal concentration polarization was found to lower both water flux and reverse salt diffusion by reducing the draw solution concentration at the interface between the support and dense layers of the membrane. Draw solution reconcentration was evaluated using reverse osmosis (RO) system design software. Analysis of experimental data and model results, combined with consideration of the costs associated with the FO and RO processes showed that a small group of seven draw solutions appeared to be the most suitable. The different characteristics of these draw solutions highlighted the importance of considering the specific FO application and membrane types being used prior to selecting the most appropriate draw solution.

1. Introduction

Osmosis is the net diffusive transport of water through a selectively permeable membrane from a solution of low solute concentration (low osmotic pressure) to a solution of high solute concentration (high osmotic pressure). In osmosis, the membrane allows passage of water, but rejects almost all solute molecules and ions. From the mid 1970s, there has been growing interest in engineered applications of osmosis [1,2], one of which is the forward osmosis (FO) process. In FO, impaired water is in contact with the dense side of a semi-permeable membrane and a highly concentrated draw solution is in contact with the support side of the membrane. The draw solution is typically an aqueous solution of a low molecular weight salt [3]. In the FO process, relatively pure water is transported from the impaired water into the draw solution; the impaired water becomes concentrated and the draw solution becomes diluted. A desalination process (e.g., reverse osmosis (RO) or distillation) can be used to reconcentrate the draw solution and simultaneously produce high-quality product water. Thus, in most water treatment applications, FO is not the ultimate process but rather a high-level pretreatment process before an ultimate reconcentration/desalination process [3].

FO has been evaluated for seawater and brackish water desalination [1,2,4], wastewater concentration and reclamation [5–8], and food concentration [9–11]. FO can also be employed in conjunction with biological processes for wastewater reuse in osmotic membrane bioreactors (OMBRs) [12,13]. The main advantage of FO is that it operates at very low hydraulic pressure, has high rejection of a broad range of contaminants [12,14], and may have lower fouling propensity and/or fouling that is more reversible than in RO processes [7,15].

One key component for successful development of FO technologies is the selection of an optimal draw solution. The first criterion is that the draw solution has a higher osmotic pressure than the feed solution to produce high water flux. Water flux (J_w) in FO can be expressed by

$$J_w = A(\pi_{D,b} - \pi_{F,b}) \quad (1)$$

where A is the membrane water permeability coefficient, $\pi_{D,b}$ is the bulk osmotic pressure of the draw solution, and $\pi_{F,b}$ is the bulk osmotic pressure of the feed solution. This equation assumes that the FO membrane used is ideally impermeable to the draw solution employed [16,17]. Also, this equation describes water flux only in the absence of concentration polarization. Concentration polarization is the accumulation or depletion of solutes near the membrane surface. Because asymmetric FO membranes are comprised of a dense layer on top of a porous support layer, concentration polarization occurs externally at the feed–membrane and draw solution–membrane interfaces, and internally in the porous

* Corresponding author. Tel.: +1 775 327 2260.
E-mail address: aachilli@unr.edu (A. Achilli).

0376-7388/$ – see front matter © 2010 Elsevier B.V. All rights reserved.
doi:10.1016/j.memsci.2010.08.010

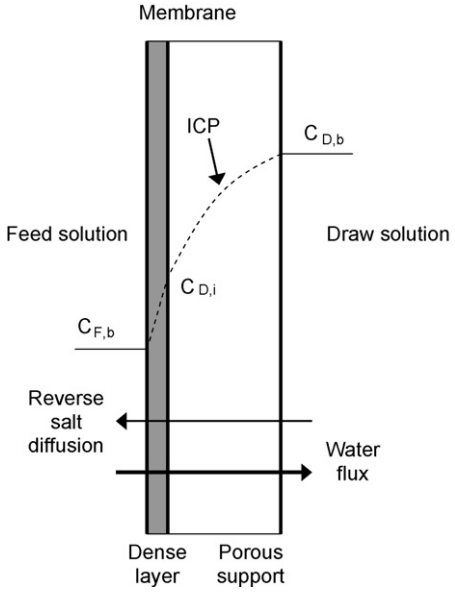

Fig. 1. Illustration of an asymmetric FO membrane with the dense layer facing the feed solution. Internal concentration polarization (ICP) within the porous support is shown; external concentration polarization is not shown because it does not occur when the feed is ultrapure water. The osmotic pressures corresponding to $C_{F,b}$, $C_{D,i}$, and $C_{D,b}$ are $\pi_{F,b}$, $\pi_{D,i}$, and $\pi_{D,b}$.

support layer of the membrane [18]. Concentration polarization results in the solute being concentrated on the feed side of the membrane and diluted inside the support layer of the membrane (Fig. 1), thus it reduces the effective osmotic pressure difference across the membrane and hence, water flux. Internal concentration polarization occurs even when ultrapure water is used as the feed solution (i.e., when $\pi_{F,b} = 0$). McCutcheon et al. [18] derived an expression that modifies Eq. (1) to include the effect of internal concentration polarization in FO applications:

$$J_w = A(\pi_{D,b} \exp(-J_w K)) \tag{2}$$

The exponent term in Eq. (2) is defined as the dilutive internal concentration polarization modulus:

$$\exp(-J_w K) = \frac{\pi_{D,i}}{\pi_{D,b}} \tag{3}$$

where $\pi_{D,i}$ is the osmotic pressure of the draw solution at the interface between the dense and support layers of the membrane and is referred to as the effective draw solution osmotic pressure. Similarly, the effective draw solution concentration is the concentration at the interface between the dense and support layer of the membranes ($C_{D,i}$ in Fig. 1) and is calculated utilizing Eq. (3) assuming that $C_{D,i}/C_{D,b} = \pi_{D,i}/\pi_{D,b}$ [19]. The solute resistivity to diffusion within the porous support layer (K) is defined by

$$K = \frac{t\tau}{D\varepsilon} \tag{4}$$

where t, τ, and ε are the thickness, tortuosity, and porosity of the support layer, respectively, and D is the diffusion coefficient of the draw solution. The term $t\tau/\varepsilon$ is often referred to as the membrane structural parameter (S) [20]. Eq. (4) can be then be expressed as

$$K = \frac{S}{D} \tag{5}$$

Recent investigations have established that internal concentration polarization is a major factor in limiting water flux in osmotically driven membrane processes [18,21,22]. There is agreement that internal concentration polarization is influenced by the structure (thickness, tortuosity, and porosity) of the membrane support layer [18,21]. However, there is not unanimous agreement as to whether internal concentration polarization is influenced by the diffusion coefficient of the draw solution. McCutcheon and Elimelech [18] improved a model that was initially developed by Lee et al. [23] in which the solution diffusion coefficient and the membrane support layer characteristics contribute to internal concentration polarization, while Tan and Ng [21] suggest that only the membrane characteristics influence water flux. In both investigations, NaCl was the only draw solution evaluated, and therefore, it was not possible to decisively determine the role of the draw solution diffusion coefficient.

The second criterion in the selection of an optimal draw solution is that the reverse diffusion of the draw solution is minimal. Similar to RO, trace quantities of salts diffuse through the membrane from the feed solution into the draw solution. However, in osmotically driven membrane processes, salts also diffuse from the draw solution into the feed solution [24]. This reverse salt diffusion occurs because of the large difference in solute concentration between the draw solution and the feed solution. The diffusion of solutes (J_s) through a semi-permeable membrane is described by Fick's Law [16]:

$$J_s = B\,\Delta C \tag{6}$$

where B is the solute permeability coefficient and ΔC is the solute concentration difference across the membrane.

Reverse salt diffusion reduces the driving force and may contaminate the feed solution. For example, if FO is used in food concentration, reverse salt diffusion can degrade the quality of the concentrated product, and if FO is used in desalination, reverse salt diffusion could have an impact on the disposal of the concentrate stream. In the OMBR process, reverse salt diffusion could inhibit or have toxic effects on the microbial community in the bioreactor, although preliminary results have shown that this is not likely [12]. While numerous FO investigations have focused on attainable water fluxes as a function of the draw solution composition and concentration, only few studies [12,13,24] have reported data on reverse salt diffusion into the feed solution and its dependence on membrane characteristics and draw solution composition.

Another important criterion in some FO applications is the availability of a suitable process for effective reconcentration of the draw solution after it has been diluted. The reconcentration process should achieve high recovery of the draw solution to minimize losses, be affordable, and be able to produce high-quality product water. For example, when considering FO for production of potable water, it is important that draw solutes are not present in the final product water, and if trace concentrations are present, they must be below the drinking water maximum contaminant level [25]. Other considerations for selection of suitable draw solutions are that the solute is water-soluble, it is solid at ambient temperature and pressure, it can be safely handled, and its cost is low enough to ensure economic viability of the process.

Often, an NaCl draw solution is used because it is highly soluble, non-toxic at low concentrations, and relatively easy to reconcentrate using conventional desalination processes (e.g., RO or distillation) without risk of scaling [5,7,8,12,26]. Other chemicals have also been suggested and tested as draw solutes. Petrotos et al. [9,11] investigated the concentration of tomato juice with FO using $CaCl_2$, $Ca(NO_3)_2$, and NaCl; McCutcheon et al. [4,27] reported a method for seawater desalination using a thermolytic draw solution based on ammonia and carbon dioxide.

The objective of this investigation was to develop a protocol for the selection of optimal draw solutions and to use the protocol to determine the most appropriate draw solutions for specific FO applications using the only commercially available FO membrane at this time. The protocol includes a desktop screening process,

evaluation of water flux and reverse salt diffusion using FO experiments, and analysis of draw solution reconcentration using RO system design software [28,29]. Using this protocol, more than 500 inorganic compounds were screened, and subsequently 14 draw solutions were tested in the laboratory at three osmotic pressures (1.4, 2.8, and 4.2 MPa). Evaluation of solute diffusion through the FO and RO membranes enabled calculation of the replenishment costs for each of the draw solutions evaluated. Replenishment costs were an effective means of differentiating the draw solute candidates because the operating costs of all the candidates were identical. This is because all of the draw solutions were tested at the same osmotic pressure (2.8 MPa), and therefore, the RO reconcentration process (the energy intense part of the process) was simulated at the same hydraulic pressure. Furthermore, the large draw solution matrix in terms of both constituents and concentrations enabled insight into the role of membrane characteristics and draw solution composition on water flux and reverse salt diffusion. Specifically, the influence of concentration polarization on water flux and reverse salt diffusion was evaluated in a way not possible in previous investigations involving only one draw solution.

2. Materials and methods

2.1. Draw solution selection protocol

A flow diagram that describes the draw solution selection protocol is illustrated in Fig. 2. More than 500 inorganic compounds were initially considered.

2.1.1. Desktop screening process

The list was first shortened through a desktop screening process by eliminating compounds that are not soluble in water and that are not solid at ambient temperature and pressure. Then, the Hazardous Materials Identification System (HMIS) codes [30] of the remaining compounds were examined. The HMIS defines the health, flammability, and physical hazards of a chemical on a scale of 0–4, with 0 representing minimal hazard and 4 representing severe hazard. Candidate compounds with a ranking greater than 2 (moderate hazard) in at least one category were eliminated. Next, OLI Stream Analyzer™ (OLI Systems, Inc., Morris Plains, NJ) was used to obtain the osmotic pressure of the draw solution candidates as a function of solution concentration. Solutions with an osmotic pressure less than 1 MPa (145 psi) at saturation concentration were eliminated. Lastly, procurement costs of the compounds were evaluated. Draw solution costs were evaluated based on Fisher Scientific unit prices [31]. The specific cost of each draw solution was determined by calculating the cost of solute needed to produce one liter of draw solution with an osmotic pressure of 2.8 MPa (406 psi) (i.e., seawater osmotic pressure). Solutions with a specific cost greater than $10/L were eliminated. At the end of the selection process, 14 inorganic compounds remained on the list (Table 1).

2.1.2. Laboratory and simulation testing

The selected draw solutions were then investigated experimentally under FO conditions to quantify the water flux and reverse salt diffusion. After this, thermolytic draw solutions (i.e., NH_4HCO_3) were removed from the list because they may be efficiently reconcentrated with a thermal process [32]. Next, the remaining draw solutions were investigated theoretically (i.e., using computer simulations) under RO conditions to evaluate RO permeate concentration. It should be noted that comparison of thermal reconcentration with RO reconcentration was not considered in this study but may be interesting in future studies.

Table 1
Draw solution unit and specific costs. Unit cost was acquired from ref. [29]. Specific cost is defined as the cost of solute needed to produce 1 L of draw solution with an osmotic pressure of 2.8 MPa.

DS	Cost, $/kg	Specific cost, $/L
NaCl	15	0.53
NH_4Cl	26	0.85
$MgCl_2$	28	0.96
$NaHCO_3$	20	1.28
Na_2SO_4	8	1.28
$CaCl_2$	35	1.53
KCl	37	1.74
$KHCO_3$	32	2.1
NH_4HCO_3	45	2.38
$(NH_4)_2SO_4$	60	4.46
K_2SO_4	53	5.38
KBr	80	5.7
$Ca(NO_3)_2$	70	6.1
$MgSO_4$	52	7.35

2.2. FO membrane

A flat-sheet cellulose triacetate (CTA) membrane (membrane B in Ref. [12]) (Hydration Technology Innovations, LLC, Scottsdale, AZ) was used in all FO experiments. The physical characteristics of this specific CTA membrane are unique compared to other commercially available semi-permeable membranes and it has been determined to be the best available membrane in FO investigations of various applications [3]. The overall thickness of the membrane is approximately 50 μm and it is comprised of two layers of cellulose triacetate polymer with a polyester support mesh embedded between them [4]. The contact angle of the CTA membrane was measured to be 61° and the membrane has been found to be negatively charged at the pH of typical feed waters [14].

2.3. Solution chemistries

Certified ACS-grade salts (Fisher Scientific, Pittsburg, PA) were used to make the draw solutions. These included $CaCl_2$, $Ca(NO_2)_3$, KBr, KCl, $KHCO_3$, K_2SO_4, $MgCl_2$, $MgSO_4$, NaCl, $NaHCO_3$, Na_2SO_4, NH_4Cl, NH_4HCO_3, and $(NH_4)_2SO_4$. Ultrapure water was used as the feed solution in all experiments. For each draw solution tested, three osmotic pressures (1.4, 2.8, and 4.2 MPa (203, 406, and 609 psi)) were evaluated. For a few of the draw solutions (K_2SO_4, $MgSO_4$, and $NaHCO_3$), it was not possible to reach an osmotic pressure of 4.2 MPa due to their low solubility. The concentrations of each draw solution for each of the three osmotic pressures, together with the solubility of each solution, were determined using OLI Stream Analyzer™ (OLI Systems, Inc., Morris Plains, NJ). Diffusion coefficients of the draw solutions were calculated according to Lobo [33], Mullin and Nienow [34], and Albright et al. [35]. All the values are summarized in Table 2 for each salt concentration that was tested.

2.4. Membrane permeability characterization

A flat-sheet bench-scale RO test system was used to determine the water permeability coefficient (A) of the CTA membrane. A membrane coupon having an effective surface area of 139 cm^2 was installed in a SEPA-CF test cell (GE Osmonics, Minnetonka, MN) with the dense layer of the membrane facing the feed solution. Mesh spacers placed in the feed channel enhanced the turbulence of the ultrapure water feed stream. A high-pressure positive displacement pump (Wanner Engineering Inc., Minneapolis, MN) was used to recirculate the feed solution at 1.5 L/min.

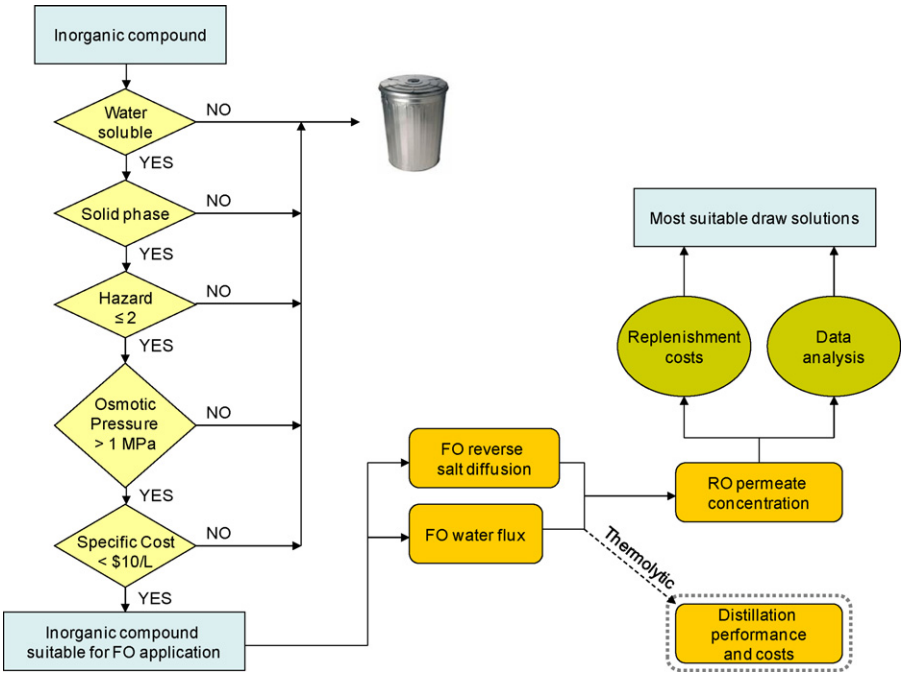

Fig. 2. Illustration of flow diagram for draw solution selection.

Table 2
Aqueous solution osmotic pressure (π_{DS}), concentration (C_{DS}), solubility, and diffusion coefficient (D).

DS	π_{DS}, MPa	C_{DS}, g/L	Solubility at 25 °C, g/L	D, 10^{-9} m^2/s
$CaCl_2$	1.4	24.3	821	1.11
	2.8	43.8		1.13
	4.2	62.3		1.15
$Ca(NO_3)_2$	1.4	42.6	1209	n.a.[a]
	2.8	87.2		n.a.
	4.2	131.2		n.a.
KBr	1.4	37.9	536	1.87
	2.8	71.3		1.9
	4.2	104.7		1.95
KCl	1.4	23.4	313	1.84
	2.8	47.0		1.86
	4.2	70.3		1.89
$KHCO_3$	1.4	32.0	200	1.26
	2.8	65.5		1.20
	4.2	99.0		1.15
K_2SO_4	1.4	49.4	105	1.11
	2.8	101.4		1.10
$MgCl_2$	1.4	20.0	466	1.04
	2.8	34.2		1.05
	4.2	47.6		1.06
$MgSO_4$	1.4	73.8	342	0.43
	2.8	141.3		0.37
NaCl	1.4	17.9	315	1.48
	2.8	35.2		1.47
	4.2	51.8		1.48
$NaHCO_3$	1.4	30.3	101	1.01
	2.8	63.9		0.96
Na_2SO_4	1.4	41.0	256	0.88
	2.8	84.7		0.76
	4.2	127.3		0.67
NH_4Cl	1.4	17.0	305	1.84
	2.8	32.6		1.87
	4.2	48.2		1.91
NH_4HCO_3	1.4	25.2	232	n.a.
	2.8	52.8		n.a.
	4.2	83.4		n.a.
$(NH_4)_2SO_4$	1.4	39.4	542	0.89
	2.8	74.3		0.95
	4.2	109.1		0.99

[a] Values not available in the literature.

The FO membrane water permeability coefficient (A) was determined using:

$$A = \frac{J_w}{\Delta\pi - \Delta P} \quad (7)$$

where $\Delta\pi$ is the osmotic pressure difference across the membrane and ΔP is the hydraulic pressure difference across the membrane. Because ultrapure water was used as the feed solution, $\Delta\pi$ was zero during the experiments. Pressure was increased in 345 kPa (50 psi) increments from 345 to 1035 kPa (50–150 psi). Pressure was held constant at each increment for a duration of 3 h. Water flux through the membrane was calculated based on the increasing weight of the permeating water on an analytical balance. The temperature was held constant at 25 °C.

2.5. FO performance experiments

FO performance was evaluated using a flat-sheet bench-scale system (Fig. 3). A CTA membrane coupon having an effective surface area of 139 cm^2 was installed in a modified SEPA cell that had symmetric channels on both sides of the membrane. This allowed for both the feed and draw solutions to flow tangential to the membrane. The membrane was oriented with the dense layer facing the feed solution. Mesh spacers placed in the feed and draw solution channels supported the membrane and enhanced mixing. Two variable-speed gear pumps (Cole-Palmer, Vernon Hills, IL) were used to recirculate the feed and draw solutions on the opposite sides of the membrane at 1.5 L/min. The temperatures of the feed and draw solutions were held constant at 25 °C and were monitored with thermocouples installed at the inlets of the test cell. The ultrapure water feed was contained in a 5.4-L constant-level reservoir; the volume was held constant by continuously replenishing the water that crossed the membrane by ultrapure water from a separate reservoir that was placed on an analytical balance linked to a computer. The draw solution was contained in a 10-L reservoir. The draw solution concentration was held constant by continuously adding concentrated draw solution to the reservoir. The pH and conductivity of the feed and draw solutions were monitored with probes placed in the feed and draw solution reservoirs.

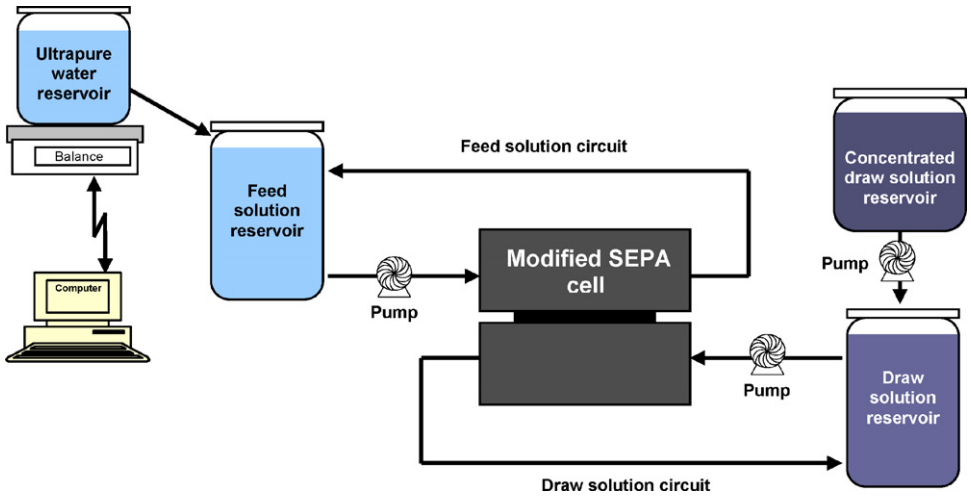

Fig. 3. Schematic of bench-scale FO system.

The FO performance for each draw solution was evaluated by determining the water flux and reverse salt diffusion. The first two columns in Table 2 represent the matrix of experiments that were performed with ultrapure water as the feed solution. For each draw solution tested, three concentrations were evaluated. Each experiment was carried out for 24 h. To quantify reverse salt diffusion, a sample of the feed solution was taken at the end of the experiment and analyzed for ion composition. Calcium, magnesium, potassium, and sodium were analyzed using an inductively coupled plasma (ICP) spectrophotometer (Perkin-Elmer, Norwalk, CT); bromide, chloride, and sulfate, using an ion chromatograph (IC) (Dionex, Sunnyvale, CA); bicarbonate using a carbon analyzer (Shidmadzu, Columbia, CO); and ammonium and nitrate using a nitrogen flow injection analysis system (Lachat, Loveland, CO).

2.6. RO reconcentration evaluation

RO reconcentration performance for each draw solution was evaluated by determining permeate concentrations using RO system design software. Reverse Osmosis System Analysis (ROSA) (Dow Filmtec, Midland, MI) [29] was used to simulate draw solution reconcentration with an SW30HRLE-4040 membrane element and IMSDesign (Hydranautics, Oceanside, CA) [28] was used to simulate draw solution reconcentration with an SWC5-4040 membrane element. These membranes are the tightest RO membranes made by the two manufacturers and they were selected because of their ability to achieve the lowest permeate concentration (i.e., the highest draw solution recovery). All simulations were performed using five RO membrane elements in series, at a feed flow rate of 3.0 m^3/h (13 gpm), and with a system recovery of 35%. The draw solutions were tested at a feed osmotic pressure of 2.8 MPa (406 psi) and a temperature of 25 °C. All of the draw solutions were evaluated with the exception of KBr because neither software included bromide in its database.

2.7. Replenishment costs evaluation

The total replenishment cost of each draw solution was calculated as the sum of the replenishment costs of the FO and RO processes. In the FO process, the replenishment cost was calculated as the product of the specific reverse salt diffusion (J_s/J_w) (which represents the amount of solute lost from the draw solution into the feed stream per unit volume of water that passes through the FO membrane into the draw solution) and the unit cost of the solute, while in the RO process the replenishment cost was calculated as the product of the RO permeate concentration and the unit cost of the solute.

3. Results and discussion

3.1. Water flux

Water flux results for each draw solution tested are summarized in Table 3. Draw solutions in Table 3 are ordered from the highest flux to the lowest flux using water flux at a draw solution osmotic pressure of 2.8 MPa (the middle value). Water fluxes ranged from 3.02×10^{-6} m/s (10.9 L/m^2 h) for KCl to 1.54×10^{-6} m/s (5.5 L/m^2 h) for $MgSO_4$ at 2.8 MPa. As anticipated, for each draw solution, water flux increases with increasing draw solution osmotic pressure. The difference in water fluxes achieved by the different draw solutions tested is solely due to internal concentration polarization effects because all the draw solutions were tested at a concentration that resulted in the same bulk osmotic pressure. Internal concentration polarization reduces the effective osmotic pressure difference across the dense layer of the membrane, and therefore, reduces water flux. The internal concentration polarization modulus (K) was calculated for each experimental condition using Eq. (2) (Table 3). The membrane structural parameter (S) was then calculated for each K using Eq. (5); this term represents the structural characteristics of the membrane support layer, and therefore, should be constant for a given membrane. Results in Fig. 4 indicate that indeed S remains reasonably constant under the different experimental conditions, thus supporting the hypothesis that internal concentration polarization is strongly dependent on D. The average S was 4.27×10^{-4} m with a standard deviation of 0.69×10^{-4} m; this represents an acceptable spread considering the uncertainties in determining D [33]. Furthermore, the S of the CTA membrane used in this investigation was found to be similar to the S of a thin-film composite membrane recently developed for FO applications (4.92×10^{-4} m) [20].

3.2. Reverse salt diffusion

Reverse salt diffusion (J_s) is summarized in Table 4 for the different experimental conditions. Draw solutions are ordered in Table 4 by magnitude of reverse salt diffusion – from the lowest to the highest solute diffusion at a draw solution osmotic pressure of 2.8 MPa. Reverse salt diffusion ranged from 1.2 g/m^2 h for $MgSO_4$ to 22.0 g/m^2 h for KBr at 2.8 MPa. As anticipated, reverse salt diffusion decreases with decreasing draw solution concentration

Table 3
Water flux (J_w), solute resistivity (K), and membrane structural parameter (S) for each draw solution tested.

DS	C_{DS}, g/L	π_{DS}, MPa	J_w, 10^{-6} m/s	K, 10^5 s/m	S, 10^{-4} m
KCl	70.3	4.2	3.74	2.37	4.48
	47.0	2.8	3.02	2.3	4.28
	23.4	1.4	1.87	2.56	4.71
NH_4Cl	48.2	4.2	3.61	2.56	4.88
	32.6	2.8	2.90	2.53	4.74
	17.0	1.4	1.88	2.52	4.65
KBr	104.7	4.2	3.59	2.58	5.03
	71.3	2.8	2.84	2.67	5.07
	37.9	1.4	1.84	2.72	5.08
NaCl	50.8	4.2	3.38	2.92	4.32
	35.2	2.8	2.68	3.05	4.49
	17.9	1.4	1.73	3.25	4.8
$CaCl_2$	62.3	4.2	3.22	3.22	3.69
	43.8	2.8	2.64	3.15	3.55
	24.3	1.4	1.75	3.11	3.46
K_2SO_4	101.4	2.8	2.52	3.47	3.82
	49.4	1.4	1.74	3.19	3.54
$NaHCO_3$	63.9	2.8	2.47	3.62	3.48
	30.3	1.4	1.68	3.53	3.56
$Ca(NO_3)_2$	131.2	4.2	2.97	n.a.[a]	n.a.
	87.2	2.8	2.46	n.a.	n.a.
	42.6	1.4	1.66	n.a.	n.a.
$MgCl_2$	47.6	4.2	2.70	4.48	4.75
	33.8	2.8	2.33	4.08	4.28
	20.0	1.4	1.58	4.09	4.25
$(NH_4)_2SO_4$	109.1	4.2	2.74	4.36	4.34
	74.3	2.8	2.28	4.29	4.08
	39.4	1.4	1.65	3.82	3.41
$KHCO_3$	99.0	4.2	2.80	4.2	4.85
	65.5	2.8	2.25	4.4	5.27
	32.0	1.4	1.48	4.85	6.1
Na_2SO_4	127.3	4.2	2.56	4.93	3.32
	84.7	2.8	2.14	4.87	3.7
	41.0	1.4	1.48	4.84	4.26
NH_4HCO_3	83.4	4.2	2.85	n.a.	n.a.
	52.8	2.8	2.04	n.a.	n.a.
	25.2	1.4	1.52	n.a.	n.a.
$MgSO_4$	141.3	2.8	1.54	8.92	3.34
	73.8	1.4	1.18	7.93	3.44
				Average	4.27

[a] Values not calculated because the diffusion coefficient (D) is not available.

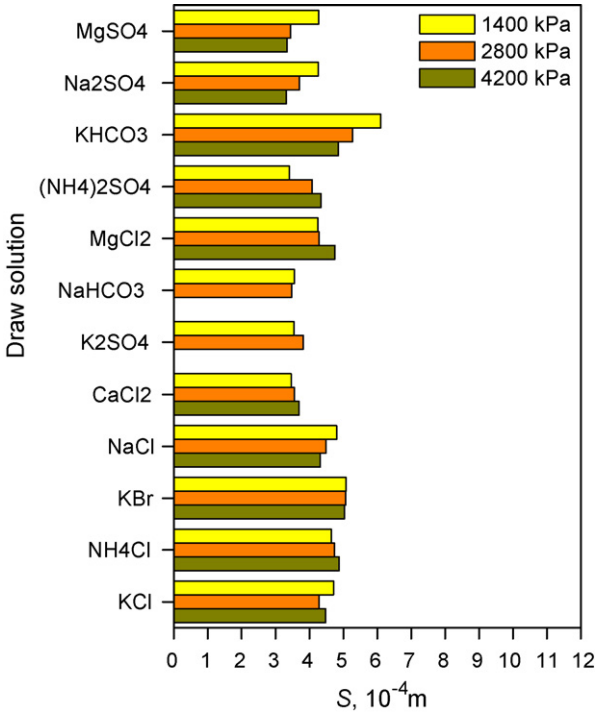

Fig. 4. S for all draw solutions tested at three different draw solution osmotic pressures and calculated for each K using Eq. (5). The average S was 4.27×10^{-4} m with a standard deviation of 0.69×10^{-4} m.

because of the decreasing driving force. Draw solutions containing larger-sized hydrated anions (i.e., $MgSO_4$, $KHCO_3$, $NaHCO_3$, Na_2SO_4, $(NH_4)_2SO_4$, and K_2SO_4) (Table 5) showed the lowest reverse salt diffusion, regardless of their paired cations. For example, Na_2SO_4 and $(NH_4)_2SO_4$ have comparable reverse salt diffusion although the ammonium cation is considerably smaller than the sodium cation. This behavior suggests that reverse salt diffusion through the negatively charged CTA membrane is likely controlled by the anion hydrated size. In these cases, in order to maintain electroneutrality, it is likely that the paired cations diffuse across the membrane at the same rate (data not shown). An exception to this behavior is NH_4HCO_3 which showed one of the highest rates of reverse salt diffusion; this behavior supports the theory of a specific affinity of the combination of the NH_4^+ and HCO_3^- ions to the CTA membrane that has been reported elsewhere [24]. KBr showed the highest reverse salt diffusion, most likely due to the smaller hydrated diameters of both potassium and bromide compared to the other ions tested (Table 5).

For each draw solution tested, the ratio between reverse salt diffusion and effective draw solution concentration ($J_s/C_{D,i}$) was calculated. Results in Table 4 indicate that for each draw solution, $J_s/C_{D,i}$ is relatively similar for the three different osmotic pressures tested. This suggests that the reverse salt diffusion through the membrane is directly proportional to the draw solution concentration difference across the membrane dense layer (which is reduced because of internal concentration polarization) and not to the difference between bulk concentrations. This behavior is in agreement with the solute transport mechanism in nonporous membranes [16].

Specific reverse salt diffusion (J_s/J_w) was also calculated and is shown in the rightmost column in Table 4. Results in Table 4 indicate that for each draw solution J_s/J_w is relatively similar for the three different osmotic pressures tested. This suggests that J_s/J_w is independent of draw solution concentration, as reported elsewhere [36]. This ratio is a useful tool to estimate how much salt is lost during the FO process. For example, for each liter of water recovered through the FO membrane at 2.8 MPa, 0.2 g of $MgSO_4$ diffuse through the membrane compared to 2.2 g of KBr. These values were used to calculate replenishment costs.

3.3. RO reconcentration evaluation

The RO permeate concentrations determined using ROSA and IMSDesign computer programs are summarized in Table 6. The average permeate concentrations were used to calculate replenishment costs. For all draw solutions, permeate concentrations using ROSA were lower than those using IMSDesign. As expected, both simulations showed higher rejection of divalent draw solutions ($MgSO_4$, $MgCl_2$, and $CaCl_2$) and relatively lower rejection of solutions containing bicarbonate ($KHCO_3$ and $NaHCO_3$) and solutions containing potassium (KCl and $KHCO_3$), with the lowest being $KHCO_3$. The most notable difference between the two software outputs was when simulating compounds containing sulfates and nitrates; in these cases, IMSDesign predicted higher permeate concentrations of these compounds, suggesting that the SWC5-4040 membrane may have higher permeability to nitrates and sulfates and/or that the programs may use different calculations.

3.4. Analysis of performance parameters

Three parameters were used to evaluate the performance of the draw solutions tested. Water flux, reverse salt diffusion, and RO

Table 4
Reverse salt diffusion (J_s), water flux (J_w), effective osmotic pressure ($\pi_{D,i}$), effective draw solution concentration ($C_{D,i}$), ratio between reverse salt diffusion and effective draw solution concentration ($J_s/C_{D,i}$), and specific reverse salt diffusion (J_s/J_w). $\pi_{D,i}$ was calculated using Eq. (3) and subsequently $C_{D,i}$ was calculated using OLI Stream Analyzer™.

DS	C_{DS}, g/L	π_{DS}, MPa	J_s, g/m^2 h	J_w, 10^{-6} m/s	$\pi_{D,i}$, kPa	$C_{D,i}$, g/L	$J_s/C_{D,i}$, (g/m^2 h)/(g/L)	J_s/J_w, g/L
$MgSO_4$	141.3	2.8	1.2	1.54	711	37.2	0.03	0.21
	73.8	1.4	0.9	1.18	548	28.2	0.03	0.22
$KHCO_3$	99.0	4.2	2.0	2.80	1296	29.5	0.07	0.20
	65.5	2.8	1.4	2.25	1042	23.5	0.06	0.17
	32.0	1.4	0.8	1.48	684	14.9	0.05	0.14
$NaHCO_3$	63.9	2.8	1.7	2.47	1145	24.2	0.07	0.19
	30.3	1.4	0.9	1.68	776	15.4	0.06	0.16
Na_2SO_4	127.3	4.2	3.1	2.56	1187	34.2	0.09	0.33
	84.7	2.8	2.7	2.14	989	27.9	0.10	0.36
	41.0	1.4	1.9	1.48	684	18.2	0.11	0.36
$(NH_4)_2SO_4$	109.1	4.2	3.6	2.74	1270	36.1	0.10	0.36
	74.3	2.8	3.3	2.28	1054	23.6	0.14	0.40
	39.4	1.4	2.5	1.65	765	30.8	0.08	0.43
K_2SO_4	101.4	2.8	3.7	2.52	1167	40.8	0.09	0.40
	49.4	1.4	2.3	1.74	804	27.3	0.09	0.37
$MgCl_2$	47.6	4.2	5.6	2.70	1252	18.4	0.30	0.58
	33.8	2.8	4.8	2.33	1081	16.7	0.29	0.57
	20.0	1.4	3.4	1.58	733	13.0	0.26	0.59
$Ca(NO_3)_2$	131.2	4.2	6.6	2.97	1374	41.8	0.16	0.62
	87.2	2.8	6.0	2.46	1138	34.2	0.17	0.67
	42.6	1.4	3.7	1.66	767	22.2	0.17	0.63
NaCl	50.8	4.2	9.1	3.38	1565	19.9	0.46	0.75
	35.2	2.8	7.2	2.68	1239	15.8	0.45	0.74
	17.9	1.4	4.6	1.73	799	10.2	0.45	0.74
NH_4Cl	48.2	4.2	10.2	3.61	1670	20.0	0.51	0.79
	32.6	2.8	7.6	2.90	1343	16.4	0.47	0.73
	17.0	1.4	5.3	1.88	871	11.1	0.48	0.79
$CaCl_2$	62.3	4.2	9.5	3.22	1491	25.6	0.37	0.82
	43.8	2.8	7.9	2.64	1221	21.8	0.36	0.83
	24.3	1.4	4.8	1.75	812	15.9	0.30	0.76
KCl	70.3	4.2	15.3	3.74	1734	29.1	0.53	1.14
	47.0	2.8	12.3	3.02	1397	23.4	0.52	1.13
	23.4	1.4	6.8	1.87	867	14.4	0.47	1.01
NH_4HCO_3	83.4	4.2	20.6	2.85	1318	23.7	0.87	2.01
	52.8	2.8	18.2	2.04	944	16.9	1.08	2.48
	25.2	1.4	11.7	1.52	702	12.6	0.93	2.14
KBr	104.7	4.2	29.2	3.59	1662	44.2	0.66	2.26
	71.3	2.8	22.0	2.84	1313	35.9	0.61	2.15
	37.9	1.4	12.3	1.84	850	24.8	0.50	1.86

permeate concentration were each normalized to the best value obtained for that individual parameter (Table 7). The highest water flux was achieved with a KCl draw solution; therefore, the ratio $J_w/(J_w)_{KCl}$ was calculated for each draw solution. Similarly, the lowest reverse salt diffusion was achieved with a $KHCO_3$ draw solution; therefore, the ratio $(J_s)_{KHCO_3}/J_s$ was calculated for each draw solution. And the lowest RO permeate concentration was achieved with an $MgSO_4$ draw solution; therefore, the ratio $(C_{P,RO})_{MgSO_4}/C_{P,RO}$ was calculated for each draw solution. This procedure enabled the ranking of each draw solution for each parameter investigated.

In analyzing the three parameters, it can be seen that no draw solutions ranked high in all categories. Five draw solutions ranked particularly high for two of the three parameters; these were $CaCl_2$, $KHCO_3$, $MgCl_2$, $MgSO_4$, and $NaHCO_3$. $CaCl_2$ and $MgCl_2$ ranked high because of their relatively high water flux and low RO permeate concentration; $KHCO_3$ and $NaHCO_3$ because of their relatively high water flux and low reverse salt diffusion; and $MgSO_4$ because of its relatively low reverse salt diffusion and RO permeate concentration.

Table 5
Effective diameters of hydrated ions from Ref. [36].

	Hydrated diameter, 10^{-12} m
Anion	
Br^-	300
Cl^-	300
HCO_3^-	450
NO_3^-	300
SO_4^{2-}	400
Cation	
Ca^{2+}	600
K^+	300
Mg^{2+}	800
Na^+	450
NH_4^+	250

Table 6
Theoretical RO permeate concentrations. Reverse Osmosis System Analysis (ROSA) was used to simulate draw solution reconcentration with an SW30HRLE-4040 membrane element and IMSDesign was used to simulate draw solution reconcentration with an SWC5-4040 membrane element.

DS	C_{DS}, g/L	C_P (ROSA), mg/L	C_P (IMS), mg/L	C_P average, mg/L
$MgSO_4$	141.3	39.5	106.4	72.9
$MgCl_2$	33.8	53.8	111.5	82.6
$CaCl_2$	43.8	62.1	132.2	97.1
Na_2SO_4	84.7	40.6	213	126.8
$(NH_4)_2SO_4$	74.3	40.2	240.6	140.4
NaCl	35.2	127.3	179	153.2
NH_4Cl	32.6	155	184.8	169.9
K_2SO_4	101.4	50.7	307.6	179.1
KCl	47	187.9	257.4	222.7
$NaHCO_3$	63.9	199	291.6	245.3
$KHCO_3$	65.5	255	374.8	314.9
$Ca(NO_3)_2$	87.2	129.4	1135.7	632.6

Table 7
Ratios between the best draw solution and the draw solution itself for water flux, reverse salt diffusion, and RO permeate concentration. Each draw solution was evaluated at an osmotic pressure of 2800 kPa.

DS	Water flux $(J_w/(J_w)_{KCl})$	Reverse salt diffusion $((J_s)_{KHCO_3}/J_s)$	RO permeate concentration $(C_{P,RO})_{MgSO_4}/C_{P,RO}$
$CaCl_2$	0.87	0.20	0.75
$Ca(NO_3)_2$	0.81	0.25	0.12
KBr	0.94	0.08	n.a.[a]
KCl	1.00	0.15	0.33
$KHCO_3$	0.75	1.00	0.23
K_2SO_4	0.84	0.41	0.41
$MgCl_2$	0.77	0.29	0.88
$MgSO_4$	0.51	0.78	1.00
NaCl	0.89	0.18	0.48
$NaHCO_3$	0.82	0.87	0.30
Na_2SO_4	0.71	0.47	0.58
NH_4Cl	0.96	0.23	0.43
NH_4HCO_3	0.68	0.07	n.a.[b]
$(NH_4)_2SO_4$	0.75	0.41	0.52

[a] Value not available because neither RO software has bromide in its database.
[b] Value not available because RO concentration were not evaluated for NH_4HCO_3.

Table 8
Draw solution replenishment cost. FO cost is the product of the specific reverse salt diffusion (J_s/J_w) and the draw solution cost and RO cost is the product of the RO permeate concentration and the draw solution cost. Total cost is the sum of the two.

DS	FO cost, $/L	RO cost, $/L	Total cost, $/L
Na_2SO_4	0.003	0.001	0.004
$NaHCO_3$	0.004	0.005	0.009
NaCl	0.011	0.002	0.013
$KHCO_3$	0.005	0.01	0.015
$MgSO_4$	0.011	0.004	0.015
$MgCl_2$	0.016	0.002	0.018
NH_4Cl	0.019	0.004	0.023
K_2SO_4	0.021	0.009	0.031
$CaCl_2$	0.029	0.003	0.032
$(NH_4)_2SO_4$	0.024	0.008	0.033
KCl	0.042	0.008	0.05
$Ca(NO_3)_2$	0.047	0.044	0.091
NH_4HCO_3	0.111	n.a.[a]	0.111
KBr	0.172	n.a.[b]	0.172

[a] Value not available because RO concentration were not evaluated for NH_4HCO_3.
[b] Value not available because neither RO software has bromide in its database.

3.5. Draw solution costs

From the desktop evaluation, specific draw solution costs ranged from 0.53 to 7.35 $/L for a draw solution having an osmotic pressure of 2.8 MPa (Table 1). This cost can be considered as an initial capital investment cost because the draw solution is continuously circulated between the FO and RO systems. A more important cost associated with the draw solution is the operating cost of replenishing the draw solution due to reverse salt diffusion through the FO membrane (Table 4) and salt diffusion through the RO membrane (Table 6). Draw solution replenishment costs per liter of water that crosses the membrane are summarized in Table 8. In general, FO replenishment costs are higher than RO replenishment costs due to the higher draw solution diffusion through FO membranes (rightmost column of Table 4) compared to RO membranes (rightmost column of Table 6). The total replenishment costs for the tested FO membrane and the modeled seawater RO membrane the (hybrid FO-RO system) ranged from $0.004 to $0.172 per liter of water produced. It is worth noting that this cost estimation is based on the current costs of chemicals for laboratory use and that purchasing bulk quantities of salts is expected to reduce the replenishment costs, but likely in the same ratio. The draw solution replenishment cost is an important parameter in evaluating the economic viability of the FO process because it implicitly considers FO water flux, reverse salt diffusion, and RO permeate concentration. The five draw solutions that had the lowest costs were Na_2SO_4, $NaHCO_3$, NaCl, $KHCO_3$, and $MgSO_4$; NaCl and Na_2SO_4 mainly because of their high water flux, $KHCO_3$ and $NaHCO_3$ mainly because of their low reverse salt diffusion, and $MgSO_4$ mainly because of its low RO permeate concentration.

3.6. Is there a best draw solution?

The draw solutions that ranked particularly high from the performance analysis were $CaCl_2$, $KHCO_3$, $MgCl_2$, $MgSO_4$, and $NaHCO_3$, while the draw solutions that ranked particularly high from the replenishment cost analysis were $KHCO_3$, $MgSO_4$, NaCl, $NaHCO_3$, and Na_2SO_4. Three draw solutions ($KHCO_3$, $MgSO_4$, and $NaHCO_3$) ranked high considering both criteria; they combine high performance with low replenishment costs. $CaCl_2$ and $MgCl_2$ ranked high considering the three performance parameters but not considering the replenishment costs because of their relatively high solute costs; and vice versa, NaCl and Na_2SO_4 ranked low considering the three performance parameters but high considering the replenishment costs because of their relatively low solute costs. The most important aspect to note is that the different characteristics of the seven high-ranking draw solutions highlight the importance of considering the specific application and membrane being used prior to selecting the most appropriate draw solution.

In the case of feed and draw solutions containing scale precursor ions (e.g., Ba^{2+}, Ca^{2+}, Mg^{2+}, SO_4^{2-}, and CO_3^{2-}), mineral salt scaling will likely occur on the membrane surface when the feed solution is concentrated above the solubility limits of various sparingly water-soluble minerals such as $BaSO_4$ (barite), $CaCO_3$ (calcite), $CaSO_4$ (gypsum), and $Mg(OH)_2$ (milk of magnesia) [37,38]. However, $Mg(OH)_2$, one of the main precipitates of magnesium can be formed only at pHs greater than 9 [38]; this would allow the use of $MgCl_2$ in most FO applications without the risk of scaling. Thus, use of draw solutions likely to cause scaling (i.e., $CaCl_2$, $KHCO_3$, $MgSO_4$, $NaHCO_3$, and Na_2SO_4) is limited to applications of FO involving pure feed solutions (e.g., food concentration). In these applications, $KHCO_3$ or $NaHCO_3$ may be most desirable because of their high FO water flux and low reverse salt diffusion. In typical environmental engineering applications, because of the complex ion matrix of the feed solutions, draw solutions that contain scale precursors are not recommended. Thus, $MgCl_2$ may be the best draw solution for most water and wastewater applications.

4. Conclusions

Internal concentration polarization is known to lower both water flux and reverse salt diffusion by lowering the draw solute concentration at the interface between the support and dense layers of the membrane. In this investigation, internal concentration polarization was proven to be strongly dependent on the diffusion coefficient of the draw solution. Furthermore, the large draw solution matrix, in terms of both constituents and concentrations, made it possible to quantitatively compare the effect of internal concentration polarization on water flux and reverse salt diffusion for a range of draw solutions.

From the literature, the most widely employed draw solutions for FO investigations are $CaCl_2$, $Ca(NO_3)_2$, NaCl, and a thermolytic draw solution based on ammonia and carbon dioxide, similar to NH_4HCO_3. From the draw solution selection protocol developed in this investigation it is apparent that a broader range of draw solutes should be considered for future FO applications and that $MgCl_2$, specifically, should be further investigated for environmental engineering applications. Furthermore, the protocol developed here can be used for draw solution selection as new FO membranes and draw solutions are developed and applied to new FO applications.

Acknowledgments

The authors acknowledge the support of the Department of Energy, Grant No. DE-FG02-05ER64143 and Hydration Technology Innovations, LLC (Scottsdale, AZ) for donating the FO membrane.

Nomenclature

ΔC	concentration difference across the membrane (g/L)
ΔP	hydraulic pressure difference (Pa)
$\Delta\pi$	osmotic pressure difference (Pa)
ε	porosity
$\pi_{D,b}$	osmotic pressure of the bulk draw solution (Pa)
$\pi_{D,m}$	osmotic pressure of the draw solution at the membrane surface (Pa)
$\pi_{F,b}$	osmotic pressure of the bulk feed solution (Pa)
π_{DS}	osmotic pressure of the draw solution (Pa)
τ	tortuosity
A	water permeability coefficient ((m/s)/kPa)
B	salt permeability coefficient (m/s)
$C_{D,b}$	salt concentration of the bulk draw solution (g/L)
$C_{D,m}$	salt concentration of the draw solution at the membrane surface (g/L)
C_{DS}	salt concentration of the draw solution (g/L)
$C_{F,b}$	salt concentration of the bulk feed solution (g/L)
C_P	salt concentration in RO permeate solution (g/L)
D	salt diffusion coefficient (m^2/s)
DS	draw solution
J_w	water flux (m/s)
J_s	salt diffusion (g/m^2 h)
K	internal concentration polarization mass transfer coefficient (s/m)
S	membrane structural parameter
t	thickness (m)

References

[1] R.E. Kravath, J.A. Davis, Desalination of seawater by direct osmosis, Desalination 16 (1975) 151–155.
[2] C.D. Moody, J.O. Kessler, Forward osmosis extractors, Desalination 18 (1976) 283–295.
[3] T.Y. Cath, A.E. Childress, M. Elimelech, Forward osmosis: principles, applications, and recent developments, Journal of Membrane Science 281 (2006) 70–87.
[4] J.R. McCutcheon, R.L. McGinnis, M. Elimelech, A novel ammonia-carbon dioxide forward (direct) osmosis desalination process, Desalination 174 (2005) 1–11.
[5] T.Y. Cath, S. Gormly, E.G. Beaudry, M.T. Flynn, V.D. Adams, A.E. Childress, Membrane contactor processes for wastewater reclamation in space. I. Direct osmotic concentration as pretreatment for reverse osmosis, Journal of Membrane Science 257 (2005) 85–98.
[6] T.Y. Cath, V.D. Adams, A.E. Childress, Membrane contactor processes for wastewater reclamation in space. II. Combined direct osmosis, osmotic distillation, and membrane distillation for treatment of metabolic wastewater, Journal of Membrane Science 257 (2005) 111–119.
[7] R.W. Holloway, A.E. Childress, K.E. Dennett, T.Y. Cath, Forward osmosis for concentration of anaerobic digester centrate, Water Research 41 (2007) 4005–4014.
[8] R.J. York, R.S. Thiel, E.G. Beaudry, Full-scale experience of direct osmosis concentration applied to leachate management, in: Proceedings of the Seventh International Waste Management and Landfill Symposium (Sardinia '99), Cagliari, Italy, 1999.
[9] K.B. Petrotos, P.C. Quantick, H. Petropakis, Direct osmotic concentration of tomato juice in tubular membrane-module configuration. II. The effect of using clarified tomato juice on the process performance, Journal of Membrane Science 160 (1999) 171–177.
[10] B. Jiao, A. Cassano, E. Drioli, Recent advances on membrane processes for the concentration of fruit juices: a review, Journal of Food Engineering 63 (2004) 303–324.
[11] K.B. Petrotos, P.C. Quantick, H. Petropakis, A study of the direct osmotic concentration of tomato juice in tubular membrane-module configuration. I. The effect of certain basic process parameters on the process performance, Journal of Membrane Science 150 (1998) 99–110.
[12] A. Achilli, T.Y. Cath, E.A. Marchand, A.E. Childress, The forward osmosis membrane bioreactor: a low fouling alternative to MBR processes, Desalination 239 (2009) 10–21.
[13] E.R. Cornelissen, D. Harmsen, K.F. de Korte, C.J. Ruiken, H. Jian-Jun Qin, L.P. Oo, Wessels, Membrane fouling and process performance of forward osmosis membranes on activated sludge, Journal of Membrane Science 319 (2008) 158–168.
[14] J.L. Cartinella, T.Y. Cath, M.T. Flynn, G.C. Miller, K.W. Hunter, A.E. Childress, Removal of natural steroid hormones from wastewater using membrane contactor processes, Environmental Science & Technology 40 (2006) 7381–7386.
[15] B. Mi, M. Elimelech, Organic fouling of forward osmosis membranes: fouling reversibility and cleaning without chemical reagents, Journal of Membrane Science 348 (2010) 337–345.
[16] M. Mulder, Basic Principles of Membrane Technology, Kluwer Academic Publishers, Dordrecht, The Netherlands, 1991.
[17] W. Pusch, R. Riley, Relation between salt rejection r and reflection coefficient [sigma] of asymmetric cellulose acetate membranes, Desalination 14 (1974) 389–393.
[18] J.R. McCutcheon, M. Elimelech, Influence of concentrative and dilutive internal concentration polarization on flux behavior in forward osmosis, Journal of Membrane Science 284 (2006) 237–247.
[19] S. Loeb, L. Titelman, E. Korngold, J. Freiman, Effect of porous support fabric on osmosis through a Loeb–Sourirajan type asymmetric membrane, Journal of Membrane Science 129 (1997).
[20] N.Y. Yip, A. Tiraferri, W.A. Phillip, J.D. Schiffman, M. Elimelech, High performance thin-film composite forward osmosis membrane, Environmental Science & Technology 44 (2010) 3812–3818.
[21] C.H. Tan, H.Y. Ng, Modified models to predict flux behavior in forward osmosis in consideration of external and internal concentration polarizations, Journal of Membrane Science 324 (2008) 209–219.
[22] A. Achilli, T.Y. Cath, A.E. Childress, Power generation with pressure retarded osmosis: an experimental and theoretical investigation, Journal of Membrane Science 343 (2009) 42–52.
[23] K.L. Lee, R.W. Baker, H.K. Lonsdale, Membrane for power generation by pressure retarded osmosis, Journal of Membrane Science 8 (1981) 141–171.
[24] N.H. Hancock, T.Y. Cath, Solute coupled diffusion in osmotically driven processes, Environmental Science and Technology 43 (2009) 6769–6775.
[25] USEPA, EPA 816-F-09-0004, National Primary Drinking Water Regulations, 2009, http://www.epa.gov/safewater/consumer/pdf/mcl.pdf.
[26] C.R. Martinetti, A.E. Childress, T.Y. Cath, High recovery of concentrated RO brines using forward osmosis and membrane distillation, Journal of Membrane Science 331 (2009) 31–39.
[27] J.R. McCutcheon, R.L. McGinnis, M. Elimelech, Desalination by ammonia–carbon dioxide forward osmosis: influence of draw and feed solution concentrations on process performance, Journal of Membrane Science 278 (2006) 114–123.
[28] IMSDesign, Hydranautics, Oceanside, CA, 2010.
[29] Reverse Osmosis System Analysis (ROSA), Dow Filmtec, Midland, MI, 2010.
[30] National Paint and Coating Association, 2010, http://www.paint.org/hmis/index.cfm.
[31] Fisher Scientific, Fisher Scientific, 2010, http://www.fishersci.com/wps/portal/HOME.
[32] P. John, Ranck, A preliminary technical and economic investigation of sea water demineralization by ion-exchange for calcium and bicarbonate ions and their subsequent removal by thermal decomposition (1), Desalination 6 (1969) 75–85.
[33] V. Lobo, Mutual diffusion coefficients in aqueous electrolyte solutions, Pure and Applied Chemistry 65 (1993) 2613–2640.
[34] J.W. Mullin, A.W. Nienow, Diffusion coefficients of potassium sulfate in water, Journal of Chemical and Engineering Data 9 (1964) 526–527.
[35] J.G. Albright, R. Mathew, D.G. Miller, Measurement of binary and ternary mutual diffusion coefficients of aqueous sodium and potassium bicarbonate solutions at 25 degree C, Journal of Physical Chemistry 91 (1987) 210–215.
[36] W.A. Phillip, J.S. Yong, M. Elimelech, Reverse draw solute permeation in forward osmosis: modeling and experiments, Environmental Science & Technology 44 (2010) 5170–5176.
[37] C. Fritzmann, J. Lowenberg, T. Wintgens, T. Melin, State-of-the-art of reverse osmosis desalination, Desalination 216 (2007) 1–76.
[38] A. Rahardianto, J. Gao, C.J. Gabelich, M.D. Williams, Y. Cohen, High recovery membrane desalting of low-salinity brackish water: integration of accelerated precipitation softening with membrane RO, Journal of Membrane Science 289 (2007) 123–137.